X-Ray structural and gas phase studies of silver(I) perfluorinated carboxylate complexes with 2,2′-bipyridyl as potential precursors for chemical vapour deposition (CVD)†

Edward Szłyk,* Robert Szczęsny and Andrzej Wojtczak

Received 19th June 2009, Accepted 10th December 2009
First published as an Advance Article on the web 15th January 2010
DOI: 10.1039/b911741e

[Ag(CF_3COO)(bpy)] (**1**), [$Ag_2(C_2F_5COO)_2$(bpy)] (**2**) and [$Ag_2(C_3F_7COO)_2$(bpy)] (**3**) were prepared and characterized by MS-EI, ^1H, ^{13}C NMR, variable-temperature IR (VT-IR) spectroscopy (solid sample and evolved volatile species) and thermal analysis. Single-crystal X-ray diffraction data revealed the polymeric structure for [$Ag_2(C_2F_5COO)_2$(bpy)] and [$Ag_6(C_3F_7COO)_6(bpy)_4$], with bridging bpy ligand, whereas for [Ag(CF_3COO)(bpy)] the dimeric system with monodentately linked carboxylate was noted. Mass spectra analysis of (**1–3**) over 30–300 °C indicates the presence of binuclear ions $[(RCOO)Ag_2]^+$ as a main volatile particles, which can be transported in CVD process. VT-IR studies of gases evolved during the thermal decomposition process, demonstrate the presence of fluorocarbon species and CO_2 as the most abundant molecules. Thermal analysis of (**1–3**) revealed a multi-stage decomposition mechanism resulting in Ag^0 formation below 290 °C. Compounds were tested for silver metal spray pyrolysis and obtained layers were characterized by scanning electron microscopy (SEM-EDX) and XRD.

Introduction

Thermal properties and volatility of silver complexes are important features which determine their usage in fabrication of metallic thin films by the chemical vapour deposition (CVD) technique.[1] These nanolayers can be applied to produce ultra-fast optical switches, or used as components of high-temperature superconducting materials and infrared sensors.[2] Organometallics or Ag(I) complexes with β-diketonates and tertiary phosphines (PMe_3, PEt_3),[3] silylated alkenes,[4] alkynes[5] and recently carboxylates[6] are currently the most often studied CVD precursors.

The low thermal stability of Ag(I) complexes with hard oxygen donors, such as perfluorinated carboxylates, can be enhanced by a ligand which stabilizes the coordination sphere of silver(I). Secondary soft donor atoms such as P or S were widely used for this purpose, however contamination of the layers by these elements was often observed. Another way of carboxylate complexes stabilization is to use the chelating ligand, therefore 2,2-bipyridyl was chosen in the studies reported here.

Several reports on silver(I) salts with 2,2-bipyridyl (bpy) were published.[7] These complexes are air-stable, exhibit good solubility in organic solvents and for the majority of them the crystal structures were solved. Among reported compounds only [Ag(hfac)(bpy)] (hfac = hexafluoroacetylacetonate) was studied as a CVD precursor but, to the best of our knowledge, there are no reports on other Ag(I) compounds with bpy tested for this method.

Therefore we have focused our effort on the preparation of new silver(I) carboxylates complexes with bpy for further CVD studies. In order to characterise complexes as precursors the thermal decomposition and IR spectra of gases evolved in this process have been examined by variable-temperature MS and IR. Moreover, X-ray crystal structures of studied compounds have been solved and discussed.

Experimental

General

CF_3COOH (99%), C_2F_5COOH (97%) and C_3F_7COOH (98%) were purchased from Aldrich, whereas 2,2′-bipyridyl (bpy), $AgNO_3$, $NaHCO_3$ and C_2H_5OH from POCh (Poland) and were used as received.

Thermal studies (TG, DTG and DTA) were performed on a SDT 2960 TA instrument. Mass spectra were registered by a Finnigan MAT 95 spectrometer using the EI technique (heating range 30–300 °C). ^1H and ^{13}C NMR spectra in $CDCl_3$ were collected with a Varian Gemini 200 MHz and Bruker 300 MHz spectrometer against TMS. IR spectra were registered using a Perkin–Elmer 2000 FT IR spectrometer in the range 4000–400 cm^{-1}, in KBr discs. Variable-temperature IR (VT-IR) studies in the solid phase were carried out with a SPECAC (Perkin–Elmer) temperature variable cell (30–250 °C). IR spectra of vapours formed during the thermolysis of complexes and transported with the carrier gas (Ar), were measured using the equipment as reported.[8] The electron micrograph studies were carried out with a LEO 1430 VP (Cambridge Ltd) equipped with an EDX Spectrometer Quantax 200 (with XFlash 4010 detector) from Bruker AXS. X-Ray diffraction of the residues from the thermal decomposition and layers was performed by an Expert

Nicolaus Copernicus University, Faculty of Chemistry, 87 100, Toruń, Poland. E-mail: eszlyk@chem.uni.torun.pl; Fax: +48 (056) 654 24 77; Tel: +48 (056) 611 43 04

† Electronic supplementary information (ESI) available: Additional data. CCDC reference numbers 734740 (**1**), 734738 (**2**) and 734739 (**3**). For ESI and crystallographic data in CIF or other electronic format see DOI: 10.1039/b911741e

Philips diffractometer. Silver was determined argentometrically (after complex mineralization), and C, H and N by elemental microanalysis (Vario-Macro Analyser).

Synthesis

In a general procedure, complexes were obtained in the reaction of RCOOAg,[9] R = CF_3, C_2F_5 and C_3F_7 with 2,2′-bipyridyl (bpy) ligand (M : L = 1 : 1). Silver(I) salts were suspended in a water–ethanol solution (3 : 1) and then bpy was added. The solution was stirred for 4 h at room temperature, filtered and the solvent was evaporated leaving a white precipitate, which was recrystallized from ethanol.

[Ag(CF_3COO)(bpy)] (1). Anal. calcd for $C_{12}H_8Ag_1F_3N_2O_2$: C 38.2, H 2.1, Ag 28.6. Found: C 38.0, H 2.4, Ag 28.5%. IR (ν_{max} (KBr)/cm^{-1}): 1673 (ν_{asym}COO), 1555, 1477, 1417 (ν_{sym}COO), 1405, 1366, 1357, 1290. ^{1}H NMR ($CDCl_3$)/ppm: 7.51 (2 H, m), 7.99 (2 H, m), 8.18 (2 H, m), 8.77 (2 H, m). ^{13}C NMR ($CDCl_3$)/ppm: 122.0, 125.5, 138.9, 151.2, 151.6, 162.6 (q, $^2J_{CF}$ = 32.7 Hz, δCOO).

[Ag$_2$(C_2F_5COO)$_2$(bpy)] (2). Anal. calcd for $C_{16}H_8Ag_2F_{10}N_2O_4$: C 27.5, H 1.2, Ag 30.9. Found: C 27.4, H 1.4, Ag 30.8%. IR (ν_{max} (KBr)/cm^{-1}): 1674 (ν_{asym}COO), 1550, 1472, 1411 (ν_{sym}COO), 1399, 1359, 1286, 960. ^{1}H NMR ($CDCl_3$)/ppm: 7.51 (2 H, m), 7.99 (2 H, m), 8.18 (2 H, m), 8.77 (2 H, m). ^{13}C NMR ($CDCl_3$)/ppm: 121.9, 125.7, 138.9, 151.3, 151.5, 162.6 (t, $^2J_{CF}$ = 24.7 Hz, δCOO).

[Ag$_2$(C_3F_7COO)$_2$(bpy)] (3). Anal. calcd for $C_{18}H_8Ag_2F_{14}N_2O_4$: C 27.1, H 1.0, Ag 27.0. Found: C 27.1, H 1.2, Ag 27.2%. IR (ν_{max} (KBr)/cm^{-1}): 1681 (ν_{asym}COO), 1549, 1458, 1405, 1397 (ν_{sym}COO), 1364, 1045, 764 cm^{-1}. ^{1}H NMR ($CDCl_3$)/ppm: 7.51 (2 H, m), 7.99 (2 H, m), 8.18 (2 H, m), 8.77 (2 H, m). ^{13}C NMR ($CDCl_3$)/ppm: 122.1, 125.6, 138.9, 151.5, 163.0 (t, $^2J_{CF}$ = 25.4 Hz, δCOO).

Crystal structure determination

Colourless crystals of (**1–3**) were obtained by recrystallization from ethanol solutions. The X-ray data were collected with an Oxford Sapphire CCD diffractometer using Mo Kα radiation λ = 0.71073 Å, by $\omega-2\theta$ method. The numerical absorption correction was applied (RED171 package of programs, Oxford Diffraction, 2000).[10] The space groups have been determined based on the systematic absences. The structures were solved by Patterson methods and refined with the full-matrix least-squares method on F^2 with the use of SHELX-97 program package.[11] For (**1**) the rotational disorder of the trifluoromethyl moiety was detected with two defined populations of 0.686/0.314 occupancy. The structure of (**1**) is similar to that reported previously by other authors.[12] In (**2**), the rotational disorder of the terminal trifluoromethyl group was detected with two populations of occupancy 0.526 and 0.474. In the structure of (**3**) the trifluoromethyl of one C_3F_7 moiety revealed the rotational disorder (two populations of 50%) and the whole C_3F_7 moiety of another ligand revealed the conformational disorder with 0.55/0.45 populations. The data collection and refinement processes of (**1–3**) are summarized in Table 3. Selected bond lengths and angles are presented in Table 4.

Table 1 Thermal analysis results

Compound	Heat effect on DTA	T/°C			Mass loss [%]	
		T_{init}	T_{max}	T_f	Calcd	Found
(**1**)	Endo	148	214	285	71.4	69.1
(**2**)	Exo	198	247	286	69.1	69.0
(**3**)	Exo	210	240	290	73.0	74.5

T_{init} = initial temperature; T_{max} = maximum temperature; T_f = final temperature.

Table 2 Mass spectra analysis data

Fragmentation ion	m/z	Compound/Temp./°C/Int.[%]				
		(**1**)		(**2**)		(**3**)
		150	300	177	300	221
[COO]$^+$	44	—	18	—	17	8
[CF_2]$^+$	50	3	13	4	12	9
[CF_3]$^+$	69	—	69	—	43	38
[C_5H_4N]$^+$	78	9	13	11	14	9
[CF_3CO]$^+$	97	—	19	—	7	—
[C_2F_4]$^+$	100	N/A	N/A	—	26	38
Ag^+	107	—	22	—	18	24
[C_2F_5]$^+$	119	N/A	N/A	—	64	13
[Ag(COO)]$^+$	147	—	—	—	20	—
[$C_{10}H_8N_2$]$^+$	156	100	100	100	100	54
[C_3F_7]$^+$	169	N/A	N/A	N/A	N/A	19
Ag_2^+	216	—	10	—	12	14
[$C_{10}H_8N_2Ag$]$^+$	263	—	1	—	1	2
[Ag_2CF_3]$^+$	284	—	11	—	—	—
[Ag_2(CF_3COO)]$^+$	329	—	99	N/A	N/A	N/A
[Ag_2(C_2F_5)]$^+$	335	—	12	—	5	—
[$C_{10}H_8N_2Ag_2$]$^+$	370	—	—	—	0,5	—
[Ag_2(C_2F_5COO)]$^+$	379	N/A	N/A	—	73	N/A
[Ag_2(CF_3COO)(CF_3)]$^+$	398	—	2	N/A	N/A	N/A
[Ag_2(C_3F_7COO)]$^+$	429	N/A	N/A	N/A	N/A	100

N/A = unable to observe; — = was not detected.

Results and discussion

IR and NMR spectra

Carboxylate ions can coordinate in many modes such as: monodentate, chelating or bridging bidentate.[13] The way of binding can be proposed by calculation of the parameter $\Delta\nu_{COO}$ = ν_{asym}COO − ν_{sym}COO for the studied compounds and comparison with the value found for analogous sodium salts.[14] In the case of [Ag(CF_3COO)(bpy)] (**1**) $\Delta\nu_{COO}$ = 256 cm^{-1} is bigger, than that for CF_3COONa ($\Delta\nu_{COO}$ = 223 cm^{-1}), what suggests the unidentate coordination of CF_3COO^-. For compounds (**2**) and (**3**) the $\Delta\nu_{COO}$ values ((**2**): 263 cm^{-1}, (**3**): 289 cm^{-1}) are comparable to $\Delta\nu$ for C_2F_5COONa = 268 cm^{-1} and C_3F_7COONa = 272 cm^{-1}, hence one can propose the bidendate coordination of carboxylates. Stretching vibrations of C=N and C=C bonds in the free bpy ligand (1579 cm^{-1} and 1553 cm^{-1})[15] are shifted upon complexation towards higher wavenumbers *ca.* 10 cm^{-1}.

^{13}C NMR spectra of (**1–3**) revealed the COO carbon line at 162.6–163.0 ppm, with the coordination shift (Δ = δCOO$_{(complex)}$ − δCOO$_{(acid)}$; 0.5, 3.4 and 3.9 ppm for (**1**), (**2**) and (**3**)) downfield in comparison to free acids. The observed Δ can be related to change of the charge on the carbonyl carbon caused by Ag–O bond formation. However the similar or even larger shifts of the COO

Table 3 Crystal data and structure refinement

	1	**2**	**3**
Empirical formula	$C_{12}H_8AgF_3N_2O_2$	$C_8H_4AgF_5NO_2$	$C_{64}H_{32}Ag_6F_{40.5}N_8O_{12}$
Formula weight	377.07	348.99	2521.70
Crystal system	Monoclinic	Monoclinic	Monoclinic
Space group	$P2_1/n$	$C2/c$	$P2_1/n$
a/Å	7.2330(10)	13.5630(10)	16.476(3)
b/Å	14.942(3)	16.1960(10)	29.367(6)
c/Å	12.034(2)	10.4560(10)	17.436(3)
α/°	90	90	90
β/°	103.78(3)	113.53(1)	103.15(3)
γ/°	90	90	90
V/Å^3	1263.1(4)	2105.9(3)	8215(3)
Z	4	8	4
D_c/Mg m^{-3}	1.983	2.202	2.039
μ/mm^{-1}	1.635	1.974	1.556
Crystal size/mm	0.37 × 0.24 × 0.12	0.60 × 0.50 × 0.20	0.17 × 0.16 × 0.07
T/K	293(2)	293(2)	292(2)
Reflections collected	12 312	10 150	37 533
Independent reflections/R_{int}	3833/0.0432	3182/0.0517	8815/0.1202
Max. and min. transmission	0.8243/0.5853	0.6935/0.3838	0.8962/0.7757
GOF on F^2	1.117	1.115	1.155
R_1 [$I > 2\sigma(I)$]	0.0428	0.0633	0.1079
wR_2 [$I > 2\sigma(I)$]	0.1031	0.1927	0.2206
Largest diffraction peak and hole/e Å^{-3}	1.180/−1.019	1.799/−1.581	1.000/−0.777

Table 4 Selected bond lengths (Å) and angles (°) for the crystal structures

$C_{12}H_8AgF_3N_2O_2$ (**1**)		$C_{64}H_{32}Ag_6F_{40.5}N_8O_{12}$ (**3**)			
Ag(1)–O(1)	2.178(2)	Ag(1)–N(1)	2.270(12)	O(1B)–Ag(2)–N(2)	93.7(5)
Ag(1)–N(1′)	2.298(3)	Ag(1)–N(3)	2.318(12)	Ag(1)–Ag(2)–Ag(3)	137.89(6)
Ag(1)–N(1)	2.323(3)	Ag(1)–O(2A)	2.349(14)	O(1C)–Ag(3)–O(2B)	107.1(5)
O(1)–Ag(1)–N(1′)	149.08(9)	Ag(2)–N(4)	2.286(12)	O(1C)–Ag(3)–O(1E)	142.5(5)
O(1)–Ag(1)–N(1)	138.35(9)	Ag(2)–O(1B)	2.342(12)	O(2B)–Ag(3)–O(1E)	108.1(5)
N(1′)–Ag(1)–N(1)	71.93(9)	Ag(2)–N(2)	2.330(12)	Ag(4)–Ag(3)–Ag(2)	109.47(5)
O(1)–Ag(1)–Ag(1)#1	116.03(7)	Ag(3)–O(1C)	2.311(13)	N(5)–Ag(4)–O(2C)	125.1(5)
N(1′)–Ag(1)–Ag(1)#1	71.07(7)	Ag(3)–O(2B)	2.354(12)	N(5)–Ag(4)–N(7)	138.2(5)
N(1)–Ag(1)–Ag(1)#1	75.76(7)	Ag(3)–O(1*E*)	2.335(13)	O(2C)–Ag(4)–N(7)	92.9(5)
C(7)–O(1)–Ag(1)	109.83(19)	Ag(4)–N(5)	2.232(13)	Ag(5)–Ag(4)–Ag(3)	135.90(6)
O(2)–C(7)–O(1)	129.6(3)	Ag(4)–O(2C)	2.342(12)	Ag(4)–Ag(5)–Ag(6)	142.36(6)
$C_8H_4AgF_5NO_2$ (**2**)		Ag(4)–N(7)	2.342(13)	Ag(5)–Ag(6)–Ag(1)#2	138.73(7)
Ag(1)–O(2)#1	2.217(4)	Ag(5)–N(8)	2.282(15)	Ag(6)#1–Ag(1)–Ag(2)–Ag(3)	158.80(9)
Ag(1)–N(1)	2.242(4)	Ag(5)–O(1D)	2.324(12)	Ag(1)–Ag(2)–Ag(3)–Ag(4)	155.44(7)
Ag(1)–O(1)	2.491(4)	Ag(5)–N(6)	2.336(11)	Ag(2)–Ag(3)–Ag(4)–Ag(5)	158.04(7)
Ag(1)–O(1)#2	2.542(4)	Ag(5)–O(2F)	2.461(19)	Ag(3)–Ag(4)–Ag(5)–Ag(6)	146.77(9)
Ag(1)–Ag(1)#3	2.8277(7)	Ag(6)–O(2D)	2.222(15)	Ag(4)–Ag(5)Ag(6)–Ag(1)#2	−132.35(10)
C(2)–C(2)#3	1.483(8)	Ag(6)–O(1A)#2	2.274(17)	N(1)–C(5)–C(6)–N(2)	−47(2)
O(2)#1–Ag(1)–N(1)	152.71(19)	Ag(6)–O(1F)	2.55(3)	N(3)–C(15)–C(16)–N(4)	−51.7(18)
O(2)#1–Ag(1)–O(1)	99.29(17)	N(1)–Ag(1)–N(3)	131.0(5)	N(5)–C(25)–C(26)–N(6)	−45(2)
N(1)–Ag(1)–O(1)	102.41(16)	N(1)–Ag(1)–O(2A)	129.4(5)	N(7)–C(35)–C(36)–N(8)	−43(2)
O(2)#1–Ag(1)–O(1)#2	105.1(2)	N(3)–Ag(1)–O(2A)	92.0(5)		
N(1)–Ag(1)–O(1)#2	95.94(15)	Ag(2)–Ag(1)–Ag(6)#1	142.04(6)		
O(1)–Ag(1)–O(1)#2	76.67(14)	N(4)–Ag(2)–O(1B)	124.7(5)		
Ag(1)–O(1)–Ag(1)#2	103.33(14)	N(4)–Ag(2)–N(2)	138.1(4)		

Symmetry codes used: $C_{12}H_8AgF_3N_2O_2$ #1 [$-x + 1, -y, -z$]; $C_8H_4AgF_5NO_2$ #1 [$-x + 1, -y, -z$] #2 [$-x + 1, -y + 1, -z$] #3 [$-x + 1, y, -z - 1/2$]; $C_{64}H_{32}Ag_6F_{40.5}N_8O_{12}$ #1 [$x - 1, y, z$] #2 [$x + 1, y, z$].

carbon signals have been reported for silver(I) aliphatic carboxylates (bidentately bonded) complexes with tertiary phosphines: [Ag(Me_3SiCH_2COO)(PPh_3)] ($\Delta = 0.2$ ppm),[16] [Ag(RCOO)(PMe_3)] (Δ = 1–2.7 ppm),[17] [Ag(RCOO)(PMe_3)$_2$] (Δ = 0.9–1.3 ppm),[18] [Ag(RCOO)(PEt_3)] (Δ = 0.6–2.7 ppm)[19] and [Ag(RCOO)(PPh_3)] ($\Delta_{\delta COO} = 2.0$–6.5 ppm).[20] Even more interesting, the chemical shifts of COO group for the non-fluorinated Ag(I) carboxylates and their complexes with tertiary phosphines were noted at lower fields (~170–180 ppm), than fluorinated.[6,21] The latter cannot be related to the inductive effect which decreases with distance, because β-substituent effect is connected rather with stereoelectronic factors. There are reports on application of ^{13}C NMR resonances for elucidation of the $RCOO^-$ group binding modes.[22] However usage of this parameter for silver(I) perfluorinated carboxylates complexes as presented above is disputable. Moreover, observed differences can also be caused by changes in the perfluorinated chain length. Considering studied compounds (**1–3**) it is evident that deshielding of COO in trifluoroacetate (**1**) complex is smaller

than for (**2**) and (**3**). Nevertheless, the observed values probably can be related to the $RCOO^-$ coordination mode. The slight variations of δCOO suggest that effect of two binding oxygen atoms have a smaller impact on tertiary carbon deshielding, than induction effects of the electronegative fluorine atoms in the nearest distance from the carbonyl group.

Decomposition studies

Thermal properties of compounds, especially the temperature of the decomposition process onset and temperature of silver formation, are significant factors for the assessment of their future usage as precursors in CVD. Results of the thermal analysis are listed in Table 1. Complex (**1**) decomposes in one endothermic process (DTA curve: Mp. = 134 °C and decomposition T_{max} = 214 °C). Experimental mass loss on TG curve for (**1**) (exp. 69.1%) does not correspond to the detachment of carboxylate and bipyridyl ligands (calcd 71.4%). This discrepancy can be related to partial formation of AgF at 500 °C. SEM-EDX analysis indicates small amount of fluorine (probably AgF), whereas at 1000 °C only Ag^0 was detected as the final product (see ESI).† Upon prolonged heating (to 1000 °C) the detected mass loss was 71.6%. Complexes (**2**) and (**3**) decompose in the one stage process (Table 1). Additional endothermic peaks which were registered on DTA curves at 183 °C for (**2**) and 120 °C for (**3**) correspond to melting points. The final product of the decomposition reactions is metallic silver, as proven by the X-ray diffractograms analysis (0.2352; 0.2026; 0.1179; 0.1444; 0.1233 nm).[23] The observed T_f for studied compounds are considerably lower than those observed for the silver(I) carboxylates (T_f = CF_3COOAg > 300 °C, C_2F_5COOAg > 400 °C, C_3F_7COOAg > 450 °C) and for [Ag(hfac)(bpy)] (T_f > 600 °C). This facts allow to assume, that compounds (**1–3**) can be promising CVD precursors below 300 °C, however their volatility at different pressure should be tested.

The variable-temperature EI-MS spectra of (**1**), (**2**) and (**3**) were recorded in the range 30–300 °C and results are listed in Table 2. In all cases the signal from $[Ag_2(RCOO)]^+$ was the most intensive and revealed the line pattern characteristic for disilver species [(3 lines, R.I. = 1 : 1.860 : 0.865, natural isotopic abundance of ^{107}Ag (51.4%) and ^{109}Ag (48.6%)]. Analogous dimeric silver species were observed in MS spectra of perfluorinated and aliphatic silver carboxylates.[24] It is noteworthy, that monomeric species of the type $[(RCOO)Ag]^+$ were not detected, except $[Ag(bpy)]^+$ ions, which exhibited low R.I.< 2%. The latter suggests that monomeric species are less stable and volatile than dimeric, due to relatively large charge of the ion and smaller number of perfluorinated residues.

In the case of (**1**) and (**2**) the fragmentation proceeds in two stages. Below 200 °C, spectra indicate detachment of N-donor ligand and its fragmentation, whereas in the second stage (above 290 °C) the fragmentation of carboxylates was also detected. In contrast the significant difference was found for (**3**), because both effects occur simultaneously in the range 200–250 °C, as presented at Scheme 1. This fact can be related to the lower stability of Ag–O bond, coming out from the stronger Lewis base character of $C_3F_7COO^-$.

Application of precursors in the CVD technique requires the determination of the thermal stability and composition of vapours, formed during thermolysis. IR spectra of (**1**), deposited on KBr plates, demonstrate the reduction of intensity of bands

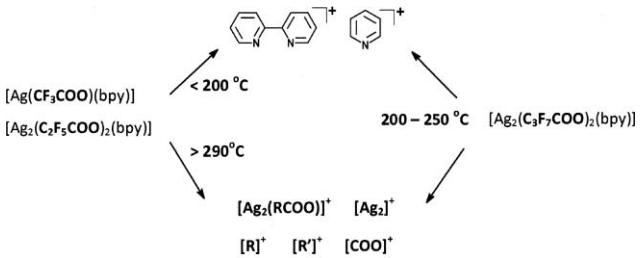

Scheme 1 MS fragmentation scheme of the analyzed complexes.

derived from 2,2′-bipyridyl ligand upon heating, whereas above 200 °C these bands disappeared. Simultaneously, the number and frequencies of the COO bands were unchanged (up to 150 °C). Besides that, spectra of vapours evolved from (**1**), registered in the range 160 and 200 °C, exhibit bands from CF_3H[25] (1151, 1376, 2328 and 3034 cm^{-1}) and CO_2 (2320 cm^{-1} and 669 cm^{-1}). The latter suggest the dissociation of carboxylate residue, followed by decarboxylation and rearrangement of the carbon chain to trifluoromethane. Simultaneously, the bands from the N-donor ligand were detected, in the spectra registered at 250 °C. That can be caused by the lower volatility of bpy and slower transport from TGA instrument *via* the heated connector to the gas cell. Therefore the bpy bands were not observed at lower temperatures, shortly after the thermal dissociation, but were noted in the VT-IR spectra registered for the solid compound.

In the case of (**2**) the asymmetric COO vibrations frequencies were shifted from 1667 to 1679 cm^{-1} over 20–250 °C (Fig. 1). Moreover, the C=O stretching band (1744 cm^{-1}) from the uncoordinated or monodentately bonded with silver(I) carboxylate group was noted above 140 °C. The absorption of this band increased, while ν_{as}(COO) = 1667 cm^{-1} reveals the opposite effect. Furthermore intensities for the bpy ligand absorptions: ν(C=N) = 1591 cm^{-1}, δ(CH) = 1007 cm^{-1} and γ(CH) = 754 cm^{-1} have decreased, while at 250 °C they have not been detected. These effects can be related to the detachment of bpy ligand below 250 °C and simultaneous rearrangement of carboxylates in the coordination sphere. For complex (**2**) the gaseous products of thermolysis were observed over 170–270 °C. When the temperature reached $T_{max.}$ = 230 °C, the intense absorption bands from C–F stretching vibrations (1100–1300 cm^{-1}) (probably C_4F_{10} is formed)[26] and bpy (1585, 1561 and 1456 cm^{-1}) were found (Fig. 2). Besides the mentioned bands, the

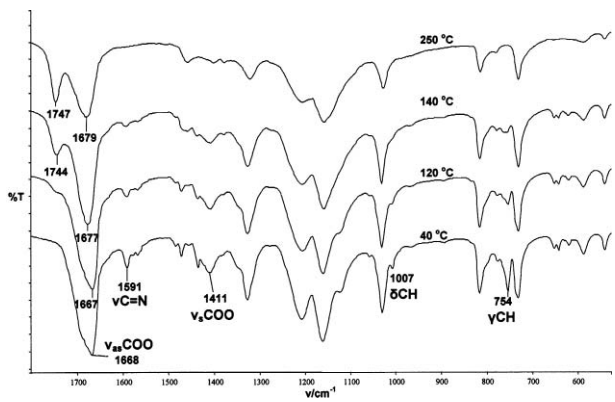

Fig. 1 Variable temperature IR spectra of (**2**), registered over 40–250 °C (solid).

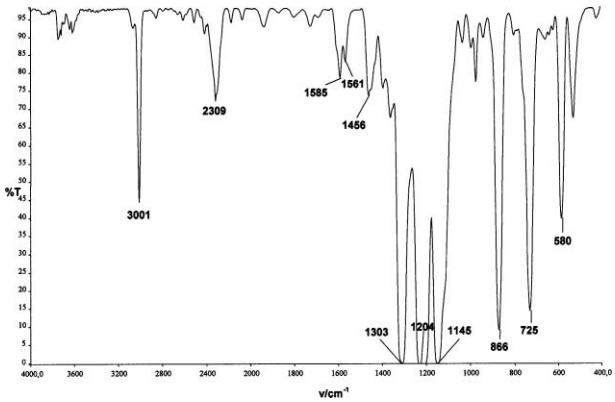

Fig. 2 VT-IR spectra of vapours formed during the thermal decomposition of (**2**) ($T = 230$ °C).

additional absorption at 2309 cm^{-1} from C≡N or/and C≡C bonds stretching vibrations of unidentified compounds were detected. Species with bidentate coordinated carboxylate ions were not observed as well.

Spectra of (**3**) registered below 110 °C, suggest the lack of structural changes, while above this temperature the bpy detachment can be noted. Simultaneously, the ν_{as}(COO) band (1668 cm^{-1}) is shifted towards higher wavenumbers (Fig. 3).[27] In the gas phase, between 160–170 °C, bands from fluorocarbon species (ν(C–F): 1140, 1183, 1232, 1268 cm^{-1}) and CO_2 (668, 2350 cm^{-1}) were observed. The COO stretching bands revealed similar changes as for (**2**), hence the presence of the monodentately bonded carboxylates in monomeric species cannot be excluded.

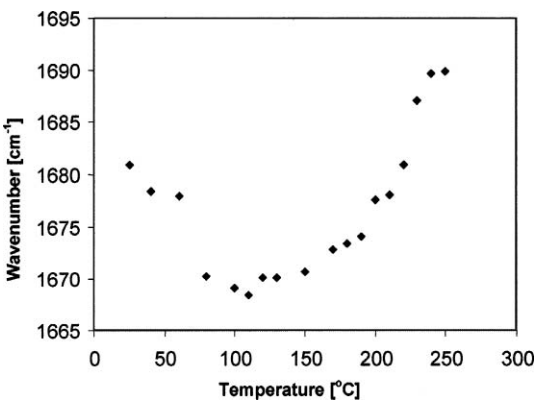

Fig. 3 Frequency of $\nu_{as(COO)}$ vibrations *vs.* temperature (**3**).

Considering our earlier studies, the comprehensive analysis, including TGA, VT-IR and EI-MS, can be used for evaluation of the suitability of compounds as precursor for (MO)CVD.[28] MS data reveal the presence of the metal binding species which can be formed in the gas phase and transported in the CVD equipment. When these metallated species exhibit sufficient stability, then they can be detected in the VT-IR spectra of vapours. According to the MS results, the silver binding species ($[Ag_2(RCOO)]^+$) were present in the gas phase. However, their thermal stability can be too low to enable their transport in the gas phase in CVD processes, hence (**1–3**) are probably not suitable for (MO)CVD.

X-Ray structure analysis

The structure of (**1**) was already reported by Bowmaker *et al.*[12] However, that structure was determined at slightly higher temperature 300 K. The comparison reveals that difference in the unit cell parameters is less than 0.1%. The asymmetric part of the structure (**1**) is formed by a Ag ion, the bipyridyl ligand and the trifluoro-acetic ion (Fig. 4), and constitutes the half of a dimer. The crystal structure is built with the centrosymmetric dimers of a formula $[Ag(CF_3COO)(bpy)]_2$. Bidentate coordination of the bipyridyl ligand is found, the Ag1–N1 and Ag1–N1′ distances being 2.323(3) and 2.298(3) Å, respectively, and the N1–Ag1–N1′ angle is 71.93(9)°, the trifluoro-acetic ligand participates in a single Ag1–O1 coordination bond of 2.178(2) Å (Fig. 4), while the second oxygen atom does not form any bond to Ag. Such molecular architecture is almost identical to that reported previously.[12] The only interaction bridging two halves of the dimer is that of Ag1–Ag1 [$-x + 1, -y, -z$] being 3.0521(9) Å. The angles between Ag1–Ag1 [$-x + 1, -y, -z$] and three coordination bonds vary between 71.07(7) and 116.03(7)° (Table 4). The AgN_2O coordination sphere is planar, with the rms deviation of fitted atoms being 0.0385 Å. The dihedral angle between that plane and the best plane of the C7–C8–O1–O2 carboxylate moiety is 12.1(2)°.

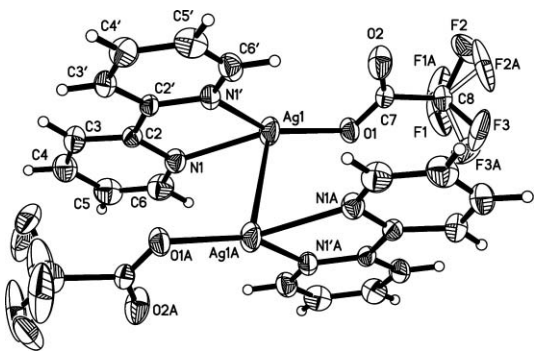

Fig. 4 Dimeric unit in the crystal structure $[Ag(CF_3COO)(bpy)]$ (**1**).

Analysis reveals the lack of packing interactions involving the CF_3 moieties. Short intermolecular contacts are detected between the chelate rings and the pyridyl rings of the adjacent molecules, the distances between the respective centers of their gravity being 3.963, 4.157 and 3.434 Å between Ag1–N1–C2–C2′–N1′ and its equivalents related by [$-x, -y, -z$] and [$1 - x, -y, -z$] and the N1–C6 [$1 - x, -y, -z$] pyridyl, respectively. The distance between centers of gravity of pyridyl rings N1–C6 and N1′–C6′[$-x, -y, -z$] is 4.277 Å. The carboxylic O2 atom, not involved in coordination of Ag1, forms an intermolecular contacts to H3A–C3[$-x, -y, -z$] and H5′A–C5′[$1/2 + x, -1/2 - y, 1/2 + z$], with the O2 ··· H3A and O2 ··· H5′A distances of 2.67 and 2.45 Å, respectively.

The CF_3 moiety reveals significant rotational disorder with two rotamers defined, and that feature seems to be characteristic for the structure reported here. That seems to result from only weak CF_3 interactions in the space available for that moiety in the crystal structure. This dynamical effect found in the crystal is consistent with the usability of the investigated compound in the CVD technique.

The asymmetric part of the structure (**2**) consists of the Ag ion, half of the bipyridyl ligand and the pentafluoropropionic anion. The rotational disorder of the terminal CF_3 group is detected

(occupancies 0.526/0.474), reflecting the lack of significant interactions involving that group in the crystal lattice.

The architecture of the reported structure might be described as a hybrid between the polymeric chain similar to that found in $[Ag(C_2F_5COO)(PMe_3)]$ and the pairs of bridging pentafluoropropionates found in $[Ag(C_2F_5COO)(PPh_3)]$, as reported by Römbke *et al.*[29] The structure is built with the polymeric chains parallel to the *Z* axis. The chain is formed by the Ag ions bridged by the bipyridyl ligands, with the N atoms coordinated to Ag, the Ag1–N1 distance being 2.242(4) Å. Two $C_2F_5COO^-$ ligands also bridge the adjacent Ag centers, with the O1 atoms forming two coordination bonds, while O2 participates in only one such bond (Fig. 5). The respective bond distances are Ag1–O1 2.491(4), Ag1–O1[$-x + 1, -y + 1, -z$] 2.542(4) and Ag1–O2 [$x, -y + 1, z - 1/2$] 2.217(4) Å. Such architecture results in a coordination sphere that could be described as strongly deformed tetrahedron. Angles within the coordination sphere vary between N1–Ag1–O1 [$-x + 1, -y + 1, -z$] of 95.9(2) and O2[$x, -y + 1, z - 1/2$]–Ag1–O1[$-x + 1, -y + 1, -z$] of 105.1(2)°. Only two of them, O1–Ag1–O1[$-x + 1, -y + 1, -z$] being 76.7(1) and O2[$x, -y + 1, z - 1/2$]–Ag1–N1 of 152.7(2) significantly deviate from the tetrahedral values. The structure reveals the short distance of 2.8276(7) Å between adjacent Ag1 and Ag1 [$-x + 1, y, -z - 1/2$] atoms. Two adjacent Ag centers and two O1 atoms related by the center of symmetry form a four-membered ring Ag1–O1–Ag1[$-x + 1, -y + 1, -z$]–O1 [$-x + 1, -y + 1, -z$]. The Ag1–O1–Ag1 and O1–Ag1–O1 angles are 103.3(1) and 76.7(1)°, respectively.

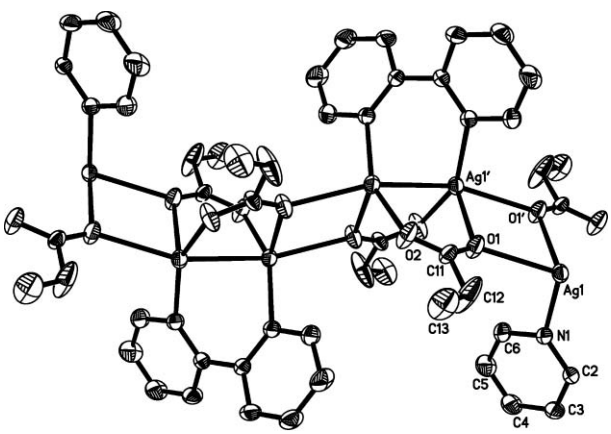

Fig. 5 Fragment of the polymeric chain of (**2**), with the numbering scheme. Fluorine and hydrogen atoms are omitted for clarity. Ag1′ and O1′ are generated from the basic coordinates with the [$-x + 1, -y + 1, -z$] transformation.

The bridging bipyridyl ligand is significantly twisted around the C2–C2 [$-x + 1, y, -z - 1/2$] bond, with the dihedral angle between the ring best planes being 41.8(2)°. The dihedral angle between two carboxylic groups bridging the adjacent Ag centers is 79.3(6)°.

Despite the significant disorder of the pentafluoropropionic moieties in the structure, the analysis revealed that they are found in the extended conformation, with the O1–C11–C12–C13 torsion angle being 175.0(1)°.

The structure obtained by the recrystallization of complex (**3**) from the ethanol solution is composed of the infinite chains based on the asymmetric part of $[Ag_6(C_3F_7COO)_6(bpy)_4]$ (Fig. 6). The asymmetric unit contains a fragment Ag1–Ag6 with four bipyridyl

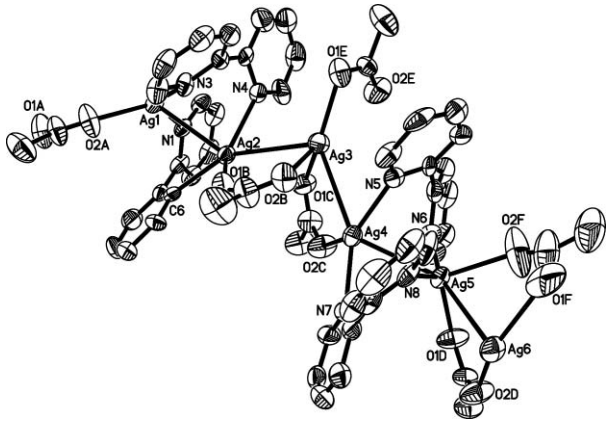

Fig. 6 Fragment of the polymeric chain of $[Ag_6(C_3F_7COO)_6(bpy)_4]$, with the numbering scheme. Fluorine and hydrogen atoms skipped for clarity.

ligands and six heptafluorobutyrate ions (Labelled with A-F letters) coordinated to the metal centers. However, the architecture of the chain is rather complicated and different for each metal center. The pairs of the neighbouring Ag centers are linked by pairs of bipyridyl bridges (Ag1–Ag2, Ag4–Ag5 or by the single carboxylate bridge (Ag2–Ag3, Ag3–Ag4, Ag6–Ag1 [$x + 1, y, z$]). All the bipyridyl ligands form the bridges linking the adjacent Ag atoms in the chain. The heptafluorobutyrate ions A-D form the bridges between the Ag atoms *via* both oxygen atoms, while carboxylates E–F are only monodentate ligands.

The coordination sphere of Ag1–Ag4 ions is formed with three Ag–O or Ag–N bonds. In particular, Ag1, Ag2 and Ag4 participate in two Ag–N and single Ag–O interactions, while Ag3 forms three bonds to the O atoms. Ag5 forms two Ag–N and two Ag–O bonds, while Ag6 interacts only with a pair of O atoms. The Ag–N distances vary from 2.232(13) Å for Ag4–N5 to 2.342(13) Å for Ag4–N7, while Ag–O distances range from 2.222(15) for Ag6–O2D to 2.55(3) for Ag6–O1F.

The angles in the coordinations sphere correspond to the strongly deformed triangular geometry for Ag1–Ag4, the angles within the coordination sphere of each Ag atom ranging from approximately 93 to 143° (Table 4). Ag5 has a strongly deformed tetrahedral coordination sphere, whereas Ag6 has a strongly deformed triangular geometry when two coordination bonds and a short contact Ag6 $\cdots$ O1F[$-1 + x, y, z$] 2.5486 Å are considered.

The puckering analysis[30] of the chelate rings formed in the structure indicated that the rings have a following conformation: envelope on Ag6 for Ag1–Ag6–O1A–C1A–O2A, an envelope on Ag6 for Ag5–Ag6–O1F–C1F–O2F, Ag5–Ag6–O2D–C1D–O1D is twisted on Ag5–Ag6, twist-boat conformation for Ag1–Ag2–N2–C6–C5–N1, twist-boat for Ag1–Ag2–N4–C16–C15–N3, screw-boat for Ag4–N5–C25–C26–N6–Ag5 and Ag4–N7–C35–C36–N8–Ag5, Ag2–Ag3–O2B–C1B–O1B is an envelope on Ag2, Ag3–Ag4–O2C–C1C–O1C is an envelope twisted on Ag3–Ag4.

Analysis revealed the metal–metal interactions along the polymeric chain with the Ag–Ag distances varying between 2.932(2) Å for Ag1–Ag2 and 3.229(2) Å for Ag2–Ag3. The Ag–Ag–Ag angles in that chain are similar to each other and range from 135.90(6)° to 142.36(6)°, for Ag5–Ag4–Ag3 and Ag4–Ag5–Ag6, respectively. Only one angle Ag4–Ag3–Ag2 of 109.487(5)° differs significantly from those mentioned above, probably due to the presence of only monodentate heptafluorobutyrate E ligand on Ag3 inserted

Table 5 Summary of deposition conditions for (**2**)

Parameter	
Concentration of solution/mg cm^{-3}	4–10
Flow rate/dm^3 min^{-1}	1–5
Carrier gas	Ar
Substrate T/°C	400
Film thickness/μm	0.2–2.5

between the carboxylate and bipyridne bridges with its carboxylic group almost perpendicular to the Ag1–Ag6 chain axis. The Ag–Ag–Ag–Ag torsion angles reflecting the rotations around Ag1–Ag2, Ag2–Ag3 and Ag3–Ag4 are almost identical and are 158.80(9), 155.44(7) and 158.04(7)°, respectively. The significant difference is found for Ag3–Ag4–Ag5–Ag6 and Ag4–Ag5–Ag6–Ag1 [$x + 1$, y, z] being 146.77(9)° and −132.35(10)°, respectively.

The bidentate coordination of bipyridyl ligands bridging the adjacent Ag centers results in their twisted conformation with the N–C–C–N torsion angles ranging from −43(2)° to −51.7(18)° for N7–C35–C36–N8 and N3–C15–C16–N4, respectively.

The heptafluoropropyl moieties of the carboxylic ligands show significant conformational disorder, what strongly affects the atomic displacement parameters. However, only for the C_3F_7 moiety of ligand B and for the CF_3 group of ligand F the alternative positions of the disordered groups could be defined. In all these cases the relative occupancy of the disordered groups is close to 50%.

Analysis of the packing interactions revealed numerous contacts between fluorine atoms of heptafluorobutyrate ligands of the adjacent chains. Also, an interaction was found between N3–C11–C12–C13–C14–C15 and N6–C26–C27–C28–C29–C30 [$-1/2 + x$, $1/2 - y$, $1/2 + z$] rings, the distance between their centers of gravity being 4.007 Å.

Results of depositions experiments

The results presented above suggest, that despite low temperature of silver formation, the studied compounds presumably are less suitable (MO)CVD precursor, than other Ag(I) complexes with phosphines or alkenes. Nevertheless, preliminary deposition experiments were carried out using horizontal *hot-wall* CVD reactor.[6c] Tests performed at moderate conditions (substrate: Si(111), $p_{evap.}$ = 300 Pa, deposition temperature: 250–300 °C) confirmed, that the volatility of the complexes (**1–3**) was not sufficient for this technique.

Series of spray pyrolysis experiments with [$Ag_2(C_2F_5COO)_2$-(bpy)] (**2**) as a precursor were performed and the obtained layers were studied with SEM and EDX methods. The complex was dissolved in $CHCl_3$ and nebulized on a silicon (111) plate, and subsequently heated at 400 °C, in the air. The procedure was repeated four times, using different concentrations of (**2**) and gas pressure in nebulizer (Table 5). The obtained coatings were non-uniform with bigger silver aggregations (Fig. 7) at the center of the plate, probably due to the solution concentration in this area. Among them silver clusters with diameter approximately 200–250 nm were formed (Fig. 8).

In the case when higher solutions concentration (10 mg cm^{-3}) and smaller argon flow rate were applied, clusters have aggregated into bigger grains (*ca.* 300–500 nm, Fig. 9). Micrographs show

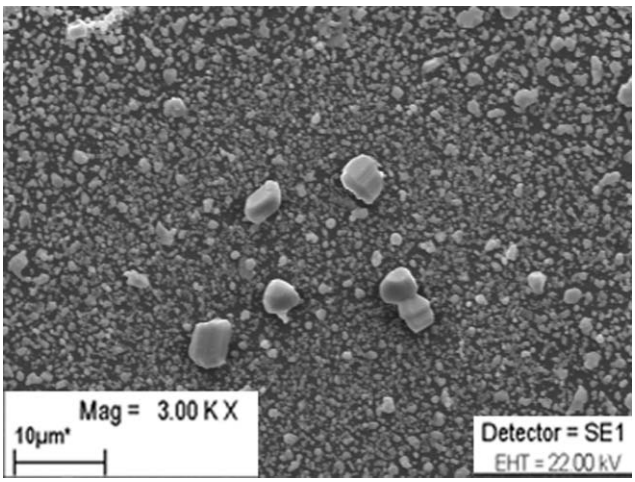

Fig. 7 SEM micrographs silver layers after thermal decomposition of [$Ag_2(C_2F_5COO)_2$(bpy)] (**2**) on Si(111).

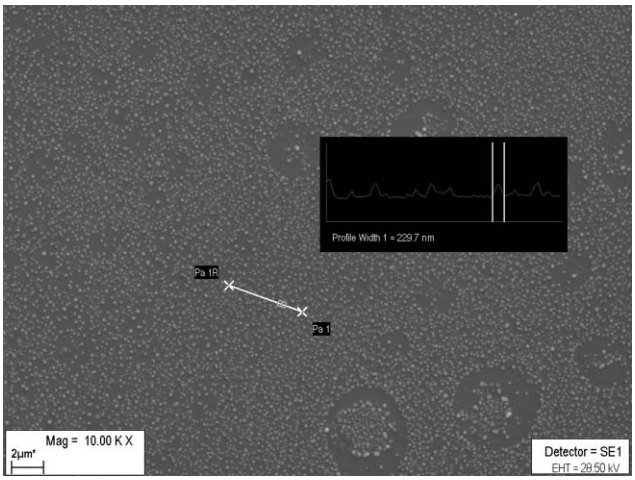

Fig. 8 SEM micrographs silver layers after thermal decomposition of [$Ag_2(C_2F_5COO)_2$(bpy)] (**2**) on Si(111) (uniform phase).

also the coalescence of these grains into the continuous sponge structures. The SEM image of the latter layer revealed spatial structures of silver nanoparticles. The results of the SEM-EDX and XRD analyses clearly indicate the presence of Ag clusters (see ESI).† Moreover, EDX spectra indicated the contamination of layers with carbon and oxygen for thinner films and the presence of fluorine in the layers of the highest thickness.

In comparison to complexes (**1–3**), the perfluorinated carboxylates and their complexes with tertiary phosphines earlier examined seem to be more convenient for (MO)CVD.[31] For example C_2F_5COOAg sublimes in the range 220–270 °C with simultaneous decomposition. The IR spectra of vapour indicate the bands at 1606 cm^{-1} derived from bridging or chelating coordinated carboxylate groups while the EI-MS measurement exhibit signals from [$Ag(C_2F_5COO)$]. In the case of [$Ag(C_2F_5COO)PMe_3$], the presence of silver carboxylate was also evident in the gas phase. Above compounds have been used as precursors and analysis demonstrated a surface with the size of metal grains in the range 0.1–1.5 μm. Similarly for [$Ag(CH_3CH_2C(CH_3)_2COO)(PEt_3)$] the volatile and stable silver–phosphine intermediates were noted during the thermal decomposition processes (MS, IR).[28b] The

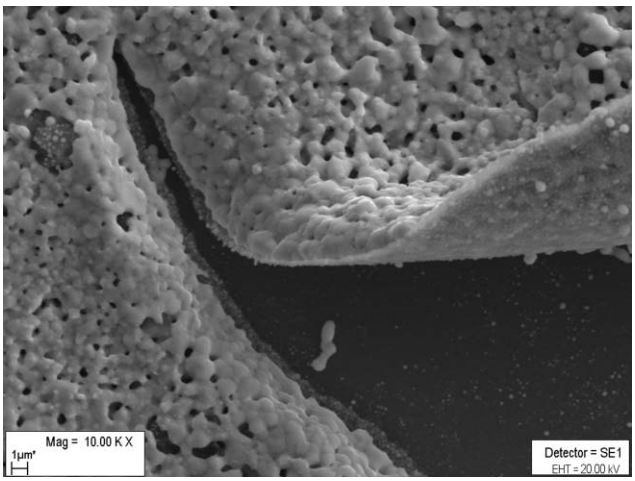

Fig. 9 SEM micrographs silver layers after thermal decomposition of $[Ag_2(C_2F_5COO)_2(bpy)]$ (**2**) on Si(111) (largest thickness).

CVD experiments with $[Ag(CH_3CH_2C(CH_3)_2COO)(PEt_3)]$ revealed deposition of nanometric silver films (thicknesses below 50 nm) at temperature 220–250 °C.

Studied compounds reveal good solubility in organic solvents (ethanol, benzene, acetonitrile and chloroform) and do not hydrolyze in water. These facts suggest the future usage of $[Ag_2(C_2F_5COO)_2(bpy)]$ as precursor in aerosol-assisted CVD (AACVD).[32]

Conclusions

Analysis of the temperature variable MS, IR and TG data revealed, that studied complexes (**1–3**) decompose below 290 °C with the formation of the metallic silver. Low pressure CVD with (**1–3**) as precursors does not provide silver layers, hence complexes were tested as precursors in aerosol assisted CVD. Single-crystal X- ray diffraction data of Ag(I) complexes with 2,2′-bipyridyl exhibit the polymeric structure of $[Ag_2(C_2F_5COO)_2bpy]$ and $[Ag_6(C_3F_7COO)_6(bpy)_4]$, with bridging bpy. Crystal data for $[Ag_2(CF_3COO)_2bpy]$ prove that it crystallizes in the dimeric architecture, with monodentately linked carboxylate. Solved structures with bridging bpy are interesting for the silver chemistry, also considering the design and synthesis of supramolecular molecules.

Acknowledgements

Authors wish to thank the Polish Ministry of Science and Higher Education for financial support grant: N204 049 31/1376.

References

1 (*a*) C. Xu, M. J. Hampden-Smith and T. T. Kodas, *Chem. Mater.*, 1995, **7**(8), 1539; (*b*) N. H. Dryden, J. J. Vittal and R. J. Puddephatt, *Chem. Mater.*, 1993, **5**, 765; (*c*) H. Schmidt, Y. Shen, M. Leschke, T. Haase, K. Kohse-Höinghaus and H. Lang, *J. Organomet. Chem.*, 2003, **25**, 669.
2 T. T. Kodas, and M. J. Hampden-Smith, *The Chemistry of Metal CVD*, Weinheim ,1994.
3 Z. Yuan, N. H. Dryen, J. J. Vittal and R. J. Puddephatt, *Chem. Mater.*, 1995, **7**, 1696.
4 K.-M. Chi, K.-H. Chen, S.-M. Peng and G.-H. Lee, *Organometallics*, 1996, **15**, 2575.
5 (*a*) K.-M. Chi and Y.-H. Lu, *Chem. Vap. Deposition*, 2001, **7**, 117; (*b*) A. Itsuki, H. Uchida, M. Satou and K. Ogi, *Nucl. Instrum. Methods Phys. Res., Sect. B*, 1997, **121**, 116.
6 (*a*) D. A. Edwards, R. M. Harker, M. F. Mahon and K. C. Molloy, *Inorg. Chim. Acta*, 2002, **328**, 134; (*b*) E. Szłyk, P. Piszczek, A. Grodzicki, M. Chaberski, A. Golinski, J. Szatkowski and T. Błaszczyk, *Chem. Vap. Deposition*, 2001, **7**, 111; (*c*) E. Szłyk, P. Piszczek, I. Łakomska, A. Grodzicki, J. Szatkowski and T. Błaszczyk, *Chem. Vap. Deposition*, 2000, **6**, 105.
7 (*a*) C. Di Nicola, Effendy, F. Marchetti, C. Pettinari, B. W. Skelton and A. H. White, *Inorg. Chim. Acta*, 2007, **360**, 1433; (*b*) C. Pettinari, J. Ngoune, B. W. Skelton and A. H. White, *Inorg. Chem. Commun.*, 2007, **10**, 329; (*c*) Effendy, F. Marchetti, C. Pettinari, B. W. Skelton and A. H. White, *Inorg. Chim. Acta*, 2007, **360**, 1424.
8 P. Piszczek, A. Grodzicki, M. Richert and A. Radtke, *Materials Science-Poland*, 2005, **23**, 663.
9 E. Szlyk, I. Lakomska and A. Grodzicki, *Thermochim. Acta*, 1993, **223**, 207.
10 CrysAlis CCD171 and RED171 package of programs, Oxford Diffraction, 2000.
11 G. M. Sheldrick, *SHELXL-97, Program for refinement of crystal structures*, University of Göttingen, Germany, 1997; G. M. Sheldrick, *SHELXS-97, Program for solution of crystal structures*, University of Göttingen, Germany, 1997.
12 G. A. Bowmaker, Effendy, S. Marfuah, B. W. Skeleton and A. H. White, *Inorg. Chim. Acta*, 2005, **358**, 4371.
13 K. Nakamoto, *Infrared and Raman Spectra of Inorganic and Coordination Compounds*, Wiley & Sons, 1978, p. 230.
14 (*a*) G. B. Deacon and R. J. Phillips, *Coord. Chem. Rev.*, 1980, **33**, 227; (*b*) G. Wilkinson, R. D. Gillard, J. A. McClaverty, *Comprehensive Coordination Chemistry*, vol. 2, Pergamon Press, NY, 1987, p. 437; (*c*) V. Robert and G. Lemercier, *J. Am. Chem. Soc.*, 2006, **128**(4), 1183.
15 (*a*) D. Czakis-Sulikowska, J. Kałużna and J. Radwańska-Doczekalska, *J. Therm. Anal. Calorim.*, 1998, **54**, 103; (*b*) D. Czakis-Sulikowska, J. Radwańska-Doczekalska, A. Czylkowska, M. Markiewicz and A. Broniarczyk, *J. Therm. Anal. Calorim.*, 2006, **86**(2), 327.
16 E. Szłyk, I. Szymańska and R. Szczęsny, *Polish J. Chem.*, 2005, **79**, 627.
17 E. Szłyk, I. Łakomska and A. Grodzicki, *Thermochim. Acta*, 1997, **303**, 41.
18 E. Szłyk and I. Łakomska, *Polish J. Chem.*, 2002, **76**, 1399.
19 E. Szłyk, I. Łakomska and A. Grodzicki, *Thermochim. Acta*, 1998, **315**, 121.
20 (*a*) E. Szłyk, I. Łakomska, A. Surdykowski and A. Goliński, *Polish J. Chem.*, 1999, **73**, 1763; (*b*) E. Szłyk, I. Łakomska and A. Grodzicki, *Polish J. Chem.*, 1994, **68**, 1529.
21 (*a*) S. W. Ng and A. H. Othman, *Acta Crystallogr., Sect. C: Cryst. Struct. Commun.*, 1997, **53**, 1393; (*b*) D. E. Edwards, M. F. Mahon, K. C. Molloy and V. Ogrodnik, *J. Mater. Chem.*, 2003, **13**, 563.
22 (*a*) R. H. Beer and S. J. Lippard, *Inorg. Chem.*, 1993, **32**, 1030; (*b*) M. Kakihana, T. Nagumo, M. Okamoto and H. Kakihana, *J. Phys. Chem.*, 1987, **91**, 6128; (*c*) B.-H. Ye, X.-Y. Li, I. D. Williams and X.-M. Chen, *Inorg. Chem.*, 2002, **41**, 6426; (*d*) S.-J. Lin, T.-N. Hong, J.-Y. Tung and J.-H. Chen, *Inorg. Chem.*, 1997, **36**, 3886.
23 *Powder Diffraction File, Sets 4-783*, International Centre for Diffraction Data (JCPDS), USA, 1977.
24 (*a*) G. D. Roberts and E. V. White, *Org. Mass Spectrom.*, 1981, **16**, 546; (*b*) S. K. Adams, D. A. Edwards and R. Richards, *Inorg. Chim. Acta*, 1975, **12**, 163.
25 *The National Institute of Standards and Technology NIST Standard Reference Database 69*, June 2005 Release, NIST Chemistry WebBook.
26 R. N. Haszeldine and K. Leedham, *J. Chem. Soc.*, 1953, 1548.
27 N. W. Alcock and V. M. Tracy, *J. Chem. Soc., Dalton Trans.*, 1976, 2243.
28 (*a*) I. B. Szymańska, P. Piszczek and E. Szłyk, *Polyhedron*, 2009, **28**, 721; (*b*) I. Szymańska, P. Piszczek, R. Szczęsny and E. Szłyk, *Polyhedron*, 2007, **26**, 2440.
29 P. Römbke, A. Schier, H. Schmidbaur, S. Cronje and H. Raubenheimer, *Inorg. Chim. Acta*, 2004, **357**, 235.
30 D. Cremer and J. A. Pople, *J. Am. Chem. Soc.*, 1975, **97**, 1354.
31 A. Grodzicki, I. Łakomska, P. Piszczek, I. Szymańska and E. Szłyk, *Coord. Chem. Rev.*, 2005, **249**, 2232.
32 (*a*) M. N. McCain, S. Schneider, M. R. Salata and T. J. Marks, *Inorg. Chem.*, 2008, **47**(7), 2534; (*b*) L. G. Hubert-Pfalzgraf and H. Guillon, *Appl. Organomet. Chem.*, 1998, **12**, 221.

